AO08: The December 2018 Methanol Plume over Siberia

Supervisor: Dr. Anu Dudhia

Alice Simmonds

Abstract

This project aims to investigate the apparent abundance of methanol over Siberia in December 2018 indicated by a Scaled Linear Retrieval (SLR) on spectra collected by the Infrared Atmospheric Sounding Interferometer (IASI) onboard the MetOp-A and MetOp-B satellites. This apparent plume of methanol is in an unlikely place and doesn't fit our understanding of the methanol cycle in the atmosphere. The brief of this project was to confirm whether or not the methanol plume exists and, either way, determine the cause of the high readings.

Preliminary tests did not support the existence of a methanol plume that could be tracked to a point source. The lack of a clear source, along with data from another research group's retrievals, called into question the reliability of the SLR. The SLR relies upon a temperature contrast between the surface and the atmosphere to give absorption features in the infrared spectrum that provide information about the gases present. In Siberia, in midwinter, this temperature contrast is greatly reduced or inverted so the uncertainty in detection increases.

To investigate why many pixels appear to contain a high concentration of methanol, we implemented the SLR on individual pixel spectra, averaged spectra, and simulated spectra. It was found that the reduced thermal contrast results in a combination of a very small methanol signature in the spectrum (of the order of instrument noise) and overcompensation of the SLR algorithm to amplify this signature.

1 Introduction

Infrared spectra obtained by the Infrared Atmospheric Sounding Interferometer (IASI) [1] instruments on the polar-orbiting MetOp satellites are rich with information about the composition of Earth's atmosphere. At Oxford, we have a variety of algorithms that can be used to retrieve atmospheric composition from this data. This investigation makes use of the Scaled Linear Retrieval (SLR) algorithm to obtain a methanol column value from a spectrum and evaluates its accuracy.

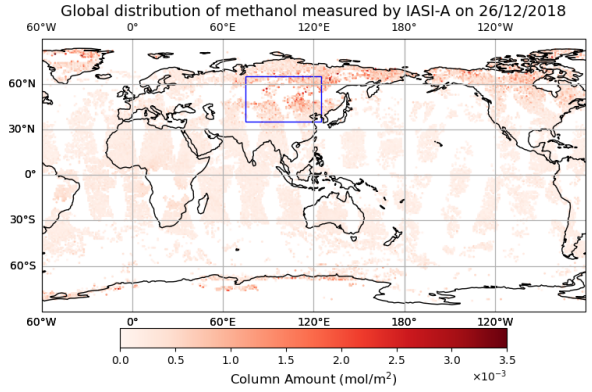

Figure 1: Methanol columns retrieved from IASI-A spectra, displayed on a 1° by 1° grid, taking the value of the median column for all the pixels in a grid-square. The blue box indicates the higher methanol concentration discussed in this work.

This work is concerned with an unusual amount of methanol (CH_3OH) appearing over Siberia in December 2018, as shown in Figure 1. The SLR algorithm detects a plume materializing across Northern Russia on 22nd December and lasting until 31st December, appearing to move south-east. This widespread abundance of methanol doesn't fit well with our understanding of the behaviour of methanol in the atmosphere so this project aims to confirm whether or not the plume exists and subsequently deduce the cause of the high methanol concentration readings.

1.1 Methanol in the atmosphere

Methanol is one of the most abundant volatile organic compounds in the atmosphere (the most abundant organic gas after methane [2]) and has an important influence on the atmospheric composition and the climate. It contributes to the formation of tropospheric ozone and other greenhouse gases so by studying its sources and distribution scientists can better understand its role in climate processes. Exposure to atmospheric methanol also has adverse health effects on humans, such as respiratory irritation and neurological damage [3], so tracking its behaviour informs policy decisions aimed at protecting human health and the environment.

1.1.1 Sources and sinks

Methanol enters Earth's atmosphere via both natural and anthropogenic processes; a major source of atmospheric methanol is the biosphere, with plants emitting methanol primarily through cell growth and during decay [4]. A study [4] modelling methanol production in

growing plants concluded that seasonal variation of atmospheric methanol is coupled with the seasonality of plant growth, with a maximum in July and a minimum during January for the Northern Hemisphere. This is supported by Figure 2 showing the global distribution of methanol detected by a retrieval run on IASI data [2]. From this, we can see that a typical retrieved value of methanol concentration for Siberia during winter ('low' methanol) hovers around 1.5×10^{16} molec cm^{-2} which corresponds to 2.5×10^{-4} mol m^{-2} (the chosen units for this report). An enhanced amount of methanol is chosen to be a concentration greater than 3.5×10^{16} molec cm^{-2}, i.e. 5.8×10^{-4} mol m^{-2}.

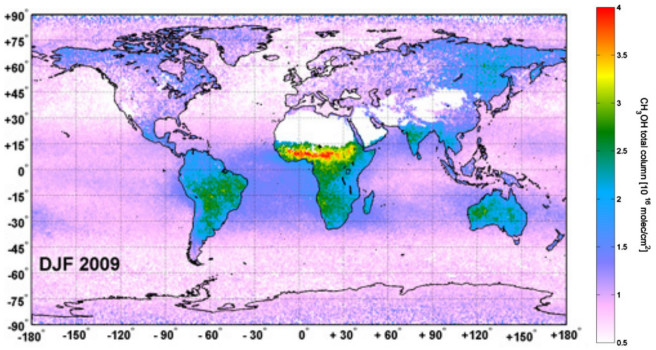

Figure 2: Column amounts of methanol averaged over December, January and February of 2009 as retrieved from IASI data by Razavi et al [2]. The white areas correspond to a filter for sandy scenes where the emissivity is uncertain.

Methanol is also produced within the atmosphere from reactions of methylperoxy radicals (CH_3O_2) with each other or with OH radicals [5], e.g.

$$CH_3O_2 + CH_3O_2 \longrightarrow CH_3OH + CH_2O + O_2 \cdot \qquad (1)$$

The burning of biofuels and biomass (through forest fires or agriculture) is another source of methanol in the lower troposphere [6]. If methanol is released in this way, we can expect to detect other gases such as carbon monoxide in a plume as well.

Industrial production of methanol for uses such as fuel, solvents, sewage treatment, and the chemical synthesis of other organic compounds also allows some methanol to enter the atmosphere.

The main removal process of methanol from the atmosphere is oxidation by OH radicals (both in the gas phase and aqueous phase in clouds), the proportion of the net flux via this pathway is indicated in Figure 3. Despite marine plants emitting a similar amount of methanol to terrestrial plants, overall the ocean is a net sink of methanol due to rapid deposition from the marine boundary layer [7]. Other sinks of methanol are wet deposition to land, meaning dissolved in precipitation, and dry deposition, referring to the turbulent mixing of gases close to the Earth's surface which then settle on moist vegetation.

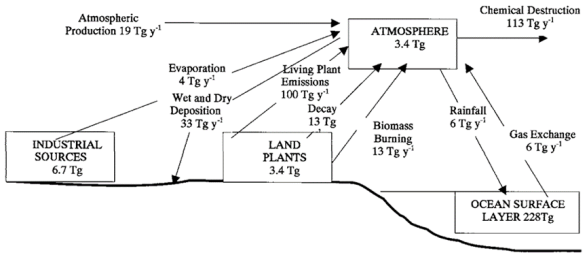

Figure 3: Atmospheric methanol cycle [4]. Boxes represent reservoirs and arrows represent fluxes, with quantities calculated as global totals.

Estimates of the lifetime of atmospheric methanol vary between 4 and 12 days, with Galbally et al. [4] estimating 8 days in 2002 and Stavrakou et al. [7] estimating 5.7 days in a more recent paper.

1.1.2 Possible plume sources

The abundance of methanol in question originates in Northern Russia in mid-December 2018 so, due to surface temperatures being significantly below 0°C, it cannot be caused by increased plant growth or decay. Forest fires or biomass burning are another possible source, but this should increase the concentration of other detectable species such as CO and CH_4 and, while it is common in Siberia during the summer months, it is unlikely in midwinter. An industrial spill seems likely, as this can be solely a methanol leak and traceable to a single point source. Additional data such as wind direction in the region and other gas retrievals should aid in determining the cause of the apparent plume.

We must also consider the possibility that the observed methanol plume is an artefact of the SLR algorithm under circumstances peculiar to this location and time period.

This report is structured as follows: Section 2 describes the satellites that measured the data and the retrieval algorithm that obtains a methanol column from the infrared spectra. Preliminary tests on the evolution of the apparent plume and their outcomes are detailed in Section 3. Section 4 explains the method used to investigate the retrieval algorithm and the results of each step of the investigation. Conclusions are drawn in Section 5.

2 Methodology

2.1 Instruments

The data used in this study is calibrated radiance spectra from the two Infrared Atmospheric Sounding Interferometers (IASI) instruments on board the MetOp-A and MetOp-B satellites. These satellites are on a near-polar, sun-synchronous orbit, so they cross the equator North to South at 9:30 am local time. This provides coverage of the whole Earth twice a day [1]. IASI is a nadir-viewing

infrared Michelson Interferometer that produces spectra for wavenumbers between 645 cm^{-1} and 2760 cm^{-1} at intervals of 0.25 cm^{-1}. These spectra can be presented as brightness temperature spectra, with a Noise Equivalent Delta Temperature (NEDT) of 0.2 K for a surface temperature of 280 K in the spectral region of interest [2]. IASI scans across-track in 30 steps, acquiring a field of view of 2 x 2 circular pixels which are 12 km in diameter (when taken at nadir) at each step position; this gives 120 across-track pixels which spans 2200 km perpendicular to its flight path. Being designed primarily for meteorology, the calibrated radiance spectra are recovered in near-real time, producing a large data volume of over a million spectra a day which are stored in the IASI L1c data product [8].

2.2 Brightness temperature spectra

2.2.1 Radiative transfer

The Earth's surface absorbs visible light (short-wave solar radiation) from the Sun and emits radiation at the infrared and microwave frequencies. Earth's surface usually has an emissivity close to 1 (although note the white spaces in Figure 2 where the emissivity of sand surfaces is uncertain) so we can model it with the Planck function, emitting a radiance $B(\nu, T)$ per unit solid angle, per unit area, per unit wavenumber. $B(\nu, T)$ is related to wavenumber ν and surface temperature T as follows:

$$B(\nu, T) = \left(\frac{2h\nu^3}{c^2}\right) \frac{1}{e^{\frac{h\nu}{kT}} - 1} \tag{2}$$

However, the radiation that reaches the satellite has been attenuated by air molecules in the atmosphere, so the intensity emerging from the top of the atmosphere is given by:

$$I_\lambda = B_0\tau_0 + \int_{\tau_0}^{1} B(\lambda, T(z))d\tau \tag{3}$$

where $\tau(\lambda)$ is the transmittance measured downwards from space, with the subscript zero referring to quantities at the Earth's surface. Assuming the atmosphere is isothermal, this integral can be performed with constant $B(T_a)$ to give the radiance seen by the satellite instrument as a weighted average of atmospheric components. The weighting is controlled by the transmittance of the atmosphere at that particular wavelength,

$$I_\lambda = B_0\tau_0 + (1 - \tau_0)B_a. \tag{4}$$

Since the effective emission temperature of the atmosphere is typically lower than the surface temperature, atmospheric gases tend to reduce the surface-emitted radiance that reaches the satellite, producing an absorption feature on the black-body spectrum of the surface,

$$\Delta B = B_0 \ - \ I_\lambda. \tag{5}$$

We often express radiance as a brightness temperature by inverting the Planck function. Brightness temperature is the temperature of a black body emitting at this measured radiance, so atmospheric absorption corresponds to a reduced brightness temperature compared to a window region (a wavelength region for which the atmosphere is transparent).

$$\Delta T = T_0 - T_I \tag{6}$$

where T_I is the brightness temperature found by inverting $I_\lambda = B(\lambda, T_I)$.

2.2.2 Methanol absorption feature

CH_3OH has an absorption feature located at 1034 cm^{-1} corresponding to the stretching frequency of the C-O bond. Detecting this using IASI is challenging because the depth of this absorption feature is small and other molecules have much stronger features in the same spectral range. The absorption features of methanol and other gases that attenuate radiation in this spectral range are shown in the upper half of Figure 4.

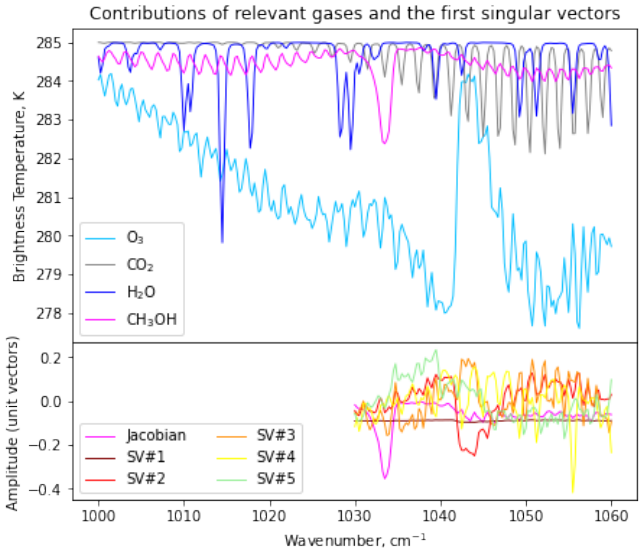

Figure 4: Absorption features of relevant atmospheric gases (upper panel). Methanol's signature has been plotted five times larger and ozone's signature has been plotted five times smaller than actual size, for ease of fitting the features in one figure. In the lower panel the Jacobian spectrum for methanol and the first few singular vectors describing a standard atmosphere are plotted over the spectral range used by the SLR, see Section 2.3. These are all normalised to a magnitude of 1.

Figure 4 was produced using a radiative transfer model called the Reference Forward Model [9] to simulate spectra for different atmospheric compositions. The model used a profile of methanol with a total column of 3×10^{-4} mol m^{-2}, since this is the typical concentration in Siberian midwinter. We also inputted typical profiles for the other relevant gases with absorption features in the same spectral range, namely CO_2, H_2O, and O_3.

As shown in Figure 4, the most notable interference with the methanol peak is ozone and the methanol signature is very small in comparison. The total column of 3×10^{-4} mol m^{-2} has a peak height of 0.5 K in the brightness temperature spectrum which is very close to the NEDT of IASI, meaning that a methanol reading is very sensitive to the instrument noise.

2.3 The Scaled Linear Retrieval

The purpose of a linear retrieval is to express the measured spectrum, $\mathbf{y}$, as a sum of n spectral components, $\mathbf{k_i}$, each weighted by a different scale factor, x_i. These spectral components are represented by the columns of the rectangular matrix $\mathbf{K}$ and the scale factors x_i fill the vector $\mathbf{x}$ such that

$$\mathbf{y} = \mathbf{K}\mathbf{x}. \tag{7}$$

A linear retrieval generates the factor $\mathbf{x}$ by which a reference profile (concentration vs altitude) of the target molecule should be multiplied in order to fit a measured spectrum. For the problem to be sufficiently linear, the absorption feature must be weak so that we can assume the peak depth is linearly correlated with concentration of the molecule. The scale factors can be 'retrieved' by finding the pseudo-inverse of $\mathbf{K}$ (since $\mathbf{K}$ is not a square matrix):

$$\mathbf{x} = \mathbf{G}\mathbf{y} = (\mathbf{K}^T\mathbf{K})^{-1}\mathbf{K}^T\mathbf{y} \tag{8}$$

The Scaled Linear Retrieval (SLR) [10] uses a combination of Jacobian spectra and Singular Vector Decomposition (SVD) to determine the columns of matrix $\mathbf{K}$.

2.3.1 Jacobian Spectrum

The Jacobian is the expected sensitivity of the measured spectrum to perturbations in physical parameters such as the surface temperature or other atmospheric profiles. The columns of matrix $\mathbf{K}$ are constructed with:

$$\mathbf{k}_i = \frac{\partial \mathbf{y}}{\partial x_i} \tag{9}$$

However, the Jacobian method requires the vector $\mathbf{x}$ to encapsulate all the atmospheric variables to characterise the spectrum, whereas SVD allows us to construct $\mathbf{K}$ with statistically determined patterns of variability within the measured spectra.

2.3.2 Singular Vector Decomposition

The columns of matrix $\mathbf{K}$ are determined using the statistical technique of Singular Vector Decomposition [11]. In this technique, a large number of spectra (100s) for different atmospheric conditions are generated using a radiative transfer model and these spectra in vector form fill the columns of a matrix $\mathbf{A}$. Matrix $\mathbf{A}$ can be decomposed into two matrices of orthonormal vectors and a diagonal matrix such that

$$\mathbf{A} = \mathbf{U}\mathbf{\Lambda}\mathbf{V}. \tag{10}$$

Here, $\mathbf{\Lambda}$ is a diagonal matrix of its eigenvalues, which can be ordered such that the components that give the largest variance are retained at the top, thus compressing the information. Matrix $\mathbf{K}$ contains columns which are the principal components of $\mathbf{A}$; they are the mutually orthogonal spectral patterns corresponding to the largest singular values in $\mathbf{\Lambda}$.

Since we are only interested in retrieving the concentration of one molecule, methanol, we produce the matrix $\mathbf{K'}$ of singular vectors for all atmospheric conditions without methanol and take the spectral signature for methanol as the vector $\mathbf{k}_m$. We model the measured spectrum as the sum of the molecular contribution $\mathbf{k}_m x_m$ and the singular vectors' contribution $\mathbf{K'x'}$:

$$\mathbf{y} = \mathbf{K}\mathbf{x} \rightarrow \mathbf{y} = (\mathbf{k}_m, \mathbf{K'}) \begin{pmatrix} x_m \\ \mathbf{x'} \end{pmatrix} \tag{11}$$

Here $\mathbf{x'}$ represents all the unknowns, apart from methanol, that contribute to the measured spectrum. The singular vectors in $\mathbf{K'}$ are fitted to several hundred simulated spectra to represent the global variability of surface temperature and atmospheric composition.

The lower panel of Figure 4 is a plot of the five most heavy-weighted singular vectors normalised to unit vectors, along with the Jacobian $\mathbf{k}_m$ of the target molecule, methanol, for the spectral range that the SLR considered. The first singular vector provides the surface temperature signature which appears as a constant unit vector in Figure 4. The peaks in the following unit vectors align with the absorption features of the gases in the atmosphere that have the largest effect on the surface brightness temperature spectrum. These are the spectral patterns that are fitted to the observed spectrum. The SLR performs a fit over this limited spectral range rather than the entire IASI spectrum to simplify the representation as much as possible.

As before, we can evaluate the pseudo-inverse $\mathbf{G}$ which can be split into the methanol and non-methanol contribution as above:

$$\mathbf{x} = \mathbf{G}\mathbf{y} \rightarrow \begin{pmatrix} x_m \\ \mathbf{x'} \end{pmatrix} = \begin{pmatrix} \mathbf{g}_m^T \\ \mathbf{G'} \end{pmatrix} \mathbf{y} \tag{12}$$

Since we only want to find x_m and don't need $\mathbf{x'}$, we can simplify this equation to:

$$x_m = \mathbf{g}_m^T\mathbf{y} \tag{13}$$

Therefore, the concentration of methanol x_m is found simply by performing a dot product of the measured spectrum $\mathbf{y}$ with a pre-determined vector $\mathbf{g}_m$.

2.3.3 Scale Factors

The SVD technique has isolated the signature of the target molecule from interfering lines and has calculated the magnitude of the signature x_m. Since the methanol signature is sufficiently small, the retrieval assumes that its amplitude is linearly related to the amount of methanol in the atmosphere.

However, for linear retrievals in the infrared, the magnitude of the Jacobian depends on the thermal contrast between the surface and the atmosphere as well as the absorber amount. Usually, the surface is warmer than the atmosphere and the molecular contributions to the spectrum appear as absorption lines, but on the rare occasions that the surface is cooler than the atmosphere they appear as emission lines. If the temperatures of the surface and the atmosphere are the same, the signatures disappear altogether, giving a magnitude x_m of zero. Within the SLR algorithm, this change due to the temperature structure is characterised by a scale factor s derived from the singular vectors.

A simplified version of the scale factor derivation is illustrated in Figure 5. This plot was generated using the Reference Forward Model again, this time modelling the atmosphere as homogeneous, with a fixed amount of CO_2 and CH_3OH, but with varying surface temperatures. Since CO_2 is well-mixed throughout the atmosphere, the scale factor by which the magnitude of the CO_2 peaks changes indicates the extent to which temperature structure has affected the amplitude of the methanol signature.

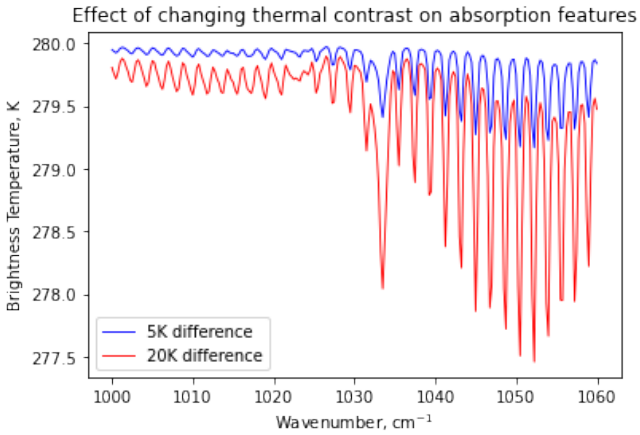

Figure 5: Sketch of the effect of surface-atmosphere thermal contrast demonstrating the need for a scale factor in the SLR. The methanol signature is the lone peak at 1034 cm^{-1} and the CO_2 signature is the numerous peaks on the right, see Figure 4 for reference. Note this is a demonstrative sketch and not spectra from a true atmosphere.

The scaled retrieval x_s is given by:

$$x_s = \frac{x_m}{s} \tag{14}$$

where the scale factor s is a linear combination of the fitted singular vector coefficients x_j:

$$s = \sum_j a_j x_j \tag{15}$$

The coefficients a_j here are obtained from a linear regression from the results of N simulated spectra, which provides a better fit for larger values of s than small values. A large scale factor s corresponds to cases where atmospheric conditions enhance the sensitivity to the target molecule, so where the temperature contrast is greatest. In these cases, the true Jacobian would be larger than the standard Jacobian.

There is a non-linear relationship between methanol column x_s and scale factor s so if s becomes very small, the amplification of an interpreted methanol signature can become very large. The IASI instrument has an NEDT of 0.2 K in the relevant spectral range so, given the methanol signature has a typical height of 0.5 K for a thermal contrast of 5 K in Figure 5, it is possible that noise in the spectra can be flagged as a methanol peak. If the surface-atmosphere temperature contrast is unfavourable, the magnitude x_m can be greatly amplified by scale factor s to give an apparent high methanol concentration x_s.

3 Preliminary investigation

To confirm the presence of a methanol plume, the SLR was run on all pixels over Siberia throughout the month of December. A filter was applied to exclude pixels with more than 10% cloud cover because clouds obscure the signatures of tropospheric molecules, causing the SLR to register low concentrations of target molecules. We also chose to restrict plots to positive values of methanol column amounts because a negative retrieval should be a result of the SLR picking up instrument noise and can therefore be neglected. Plots were created like Figure 1 for every day of December in 2018 and other years, to confirm that the plume appears on 22nd December and appears to move southwards over the course of a week. This was double-checked by running the SLR on spectra from IASI instruments on both MetOp-A and MetOp-B satellites. The plots for December 2017 confirm that it is not an annual occurrence, so this rules out the possibility of a seasonal source of methanol and leaves us with two credible sources: biomass burning and an industrial leak.

The Hybrid Single-Particle Lagrangian Integrated Trajectory model (HYSPLIT) [12] was developed by the National Oceanic and Atmospheric Administration to track air parcel trajectories. It was used to carry out backward trajectory analysis of air parcels at three different tropospheric heights, to see if the apparent abundance of atmospheric methanol can be tracked to a source. Figure 6 indicates that the plume on 26th December which we see around 50° N 110° E has no obvious source, so

it is doubtful that the methanol plume is caused by an industrial leak from a single point.
Another approach was to calculate the time evolution of the total amount of methanol over Siberia. If there were a localised and instantaneous source of the methanol, then we should have found a spike in methanol amount and an exponential decay which aligns with our knowledge of methanol's lifetime in the troposphere. No such exponential decay was visible, and the apparent plume spread out too quickly in the distribution plots to be pinned down to one point source.

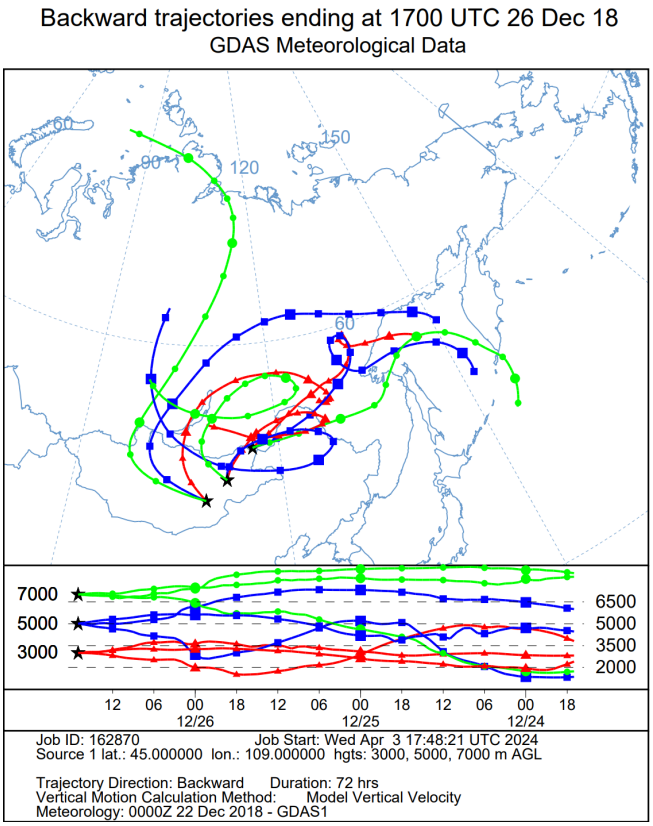

Figure 6: Backwards wind trajectory using NOAA HYSPLIT Model [12]

The lack of expected plume evolution calls into question the reliability of the SLR and suggests it could be behaving anomalously, so the SLR-produced results were compared to data provided by RAL Space's Remote Sensing Group (RSG) [13]. The RSG has its own IASI retrieval product, using a more complex algorithm than the SLR. No plume of methanol was visible when cross-checking against their retrieval for Siberia in December 2018, implying that the SLR is producing a false positive result. The multi-species retrieval also confirmed that the RSG recorded no abundance of other gases that could be emitted alongside methanol in biomass burning such as carbon monoxide, thus ruling out biomass burning as a possible source.
Turning our attention to the anomalous behaviour of the SLR, when plotting the scale factor s of each pixel in the region throughout December it was found that a low scale factor tracked the movement of the so-called methanol plume. Since our initial gridding for the plot was restricted to positive SLR values (since any negative values should be attributed to noise) it is possible that the scale factor is the sole cause of the apparent plume as it could be just amplifying noise and only the positive amplified noise is included in the plot.
All preliminary tests point to an absence of a methanol plume, and all possible plume sources have been ruled out. Given our understanding of the retrieval algorithm's sensitivity to noise and other gases with absorption features in the same spectral range, we now investigate the behaviour of the SLR algorithm. The following investigation sought to test a few possible explanations for the high methanol readings, namely, the amplified noise due to decreased scale factor, and the misinterpretation of other absorption features in the spectrum.

4 SLR algorithm investigation

Since we suspect the methanol plume is not real, we now consider why the SLR might generate high methanol column values in this particular location at this particular time. We limit our focus to the time evolution of a smaller geographical region, over which we expect little variation in atmospheric temperature structure and other gas profiles. As shown in Figure 7, the chosen region is quite far South because it is likely to be warmer than Northern Siberia so should have more favourable detection conditions, and because previous work has been published on IASI measurements of methanol over the Baikal region in Russia [6].

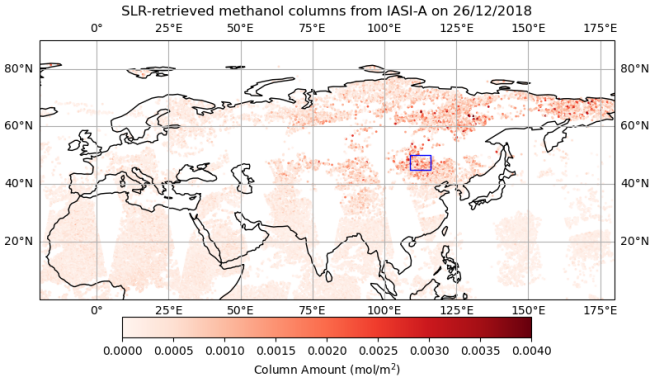

Figure 7: Methanol columns given by SLR over Siberia on 26/12/2018, with the blue box highlighting the region of high methanol concentration for closer analysis.

The chosen region of interest is the 5° x 7° box spanning latitudes 45° to 50° North and longitudes 109° to 116° East. Throughout this investigation only pixels with less than 10% cloud cover were considered, providing a sample of 300–500 pixels per day within the box.
This plot gives the methanol column of each pixel produced by implementing the SLR on the spectrum of each individual pixel. The SLR result is a combination of the

methanol signature and the scale factor; this investigation aims to separate these two components.

4.1 Scale factor variation

4.1.1 Method

The SLR was run on every individual cloud-free pixel's spectrum in the boxed region of interest for each day of December, to produce a scale factor s and column retrieval x_s for each pixel. The time evolution of the median and spread of the retrieved methanol column is plotted in green in Figure 8. This comprises the original data that this investigation calls into question.

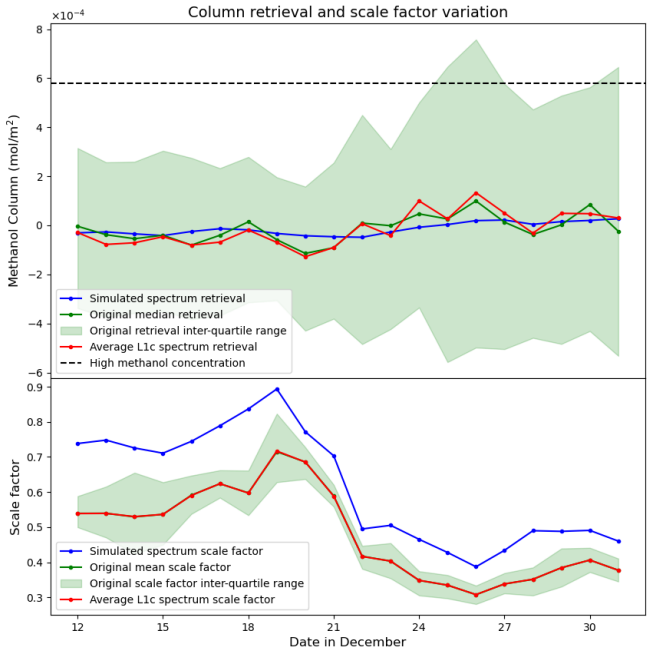

Figure 8: Variation of methanol column retrieval x_s (upper panel) and scale factor s (lower panel) with time. The median and spread of results from the original data are shown in green, with a retrieval on the average spectrum shown in red. The black dashed line indicates the chosen value of 'high' methanol concentration, and, on days of high methanol amounts, more than a quarter of the pixels contain a 'high' concentration. See Section 4.3 for an explanation of the retrieval run on simulated spectra.

Since the changing scale factor s tracks the plume's movement, we must account for a decreased scale factor amplifying instrument noise. In order to reduce instrument noise, the spectrum of each cloud-free pixel in the boxed region was extracted and averaged to give one spectrum for the region with reduced noise. As before, the SLR was run on this average spectrum to obtain a scale factor s and column x_s; these values are theoretically more accurate because, assuming temperature and gas profiles are uniform over the small area, the averaging process should reduce the instrument noise on the spectrum.

4.1.2 Results

The SLR run on individual pixels produces s and x_s values shown in green in Figure 8. The average scale factor drops from a typical value of 0.5 – 0.7 down to 0.3 at its lowest. This minimum value of the scale factor coincides with the day we retrieve the highest concentration of methanol on average, 26th December. While the median x_s increases slightly as the scale factor drops, the upper quartile shows the sharpest increase, for the final days in December more than a quarter of the readings are above our classification of a 'high' methanol concentration. Since the SLR involves a division by the scale factor given by 14, this reduced scale factor corresponds to a non-linear increase in methanol column value, i.e. a scale factor of 0.3 would give a column value more than three times greater than that perceived in the measured spectrum.
Plotted in red in Figure 8 are the s and x_s values given when running the SLR on an average spectrum for the whole region. As shown, the scale factor s behaves exactly the same; the red data points obscure the green data points in the lower panel. Since the scale factor is affected by temperature structure which remains uniform over the area of interest, it is unsurprising that averaging the spectra before running the SLR gives the same result as averaging the retrieval results. Even with reduced noise due to averaging the spectra, the methanol column is found to be higher than usual on 26th December.

4.2 Atmospheric structure

4.2.1 Method

Having confirmed the decreased scale factor on the days that the plume appears, we now investigate the other reasons the pixels might flag as 'high' methanol. It is possible that the actual atmospheric structure might be anomalous, with regard to being outside the dataset used to establish the singular vectors, plotted in Figure 4.
Eumetsat also produces an IASI Level 2 product [14] providing their retrievals of the atmospheric temperature, H_2O and O_3 profiles, and the surface temperature of each pixel. The average profiles were calculated for all the cloud-free pixels in the boxed region and plotted below. We suspect that the decreased scale factor is due to the decreased thermal contrast between the Earth's surface and the first atmospheric layer (lowest altitude).

4.2.2 Results

Figure 9 shows that the decreased scale factor is indeed caused by a cooler lower troposphere and hence a smaller thermal contrast between the surface and the atmosphere. The thermal contrast on the days plotted in red is about 5 K which corresponds to a methanol peak of 0.5 K in brightness temperature difference, see Figure

5. This is a very small feature to detect for the SLR and is close to the instrument noise value of 0.2 K.
The H_2O profiles in Figure 10 indicate that there is less water vapour in the lower troposphere on the days when methanol concentration is higher on average. This is to be expected due to the colder tropospheric temperature on these days — a cooler atmosphere will condense any water vapour present.
As seen in Figure 11, on the days flagged as high methanol, the stratospheric ozone levels are higher than the rest of the month. Since the absorption feature of ozone is much larger than methanol's peak in this spectral range, it is possible that the increase in ozone concentration is misinterpreted by the SLR as a higher methanol concentration.

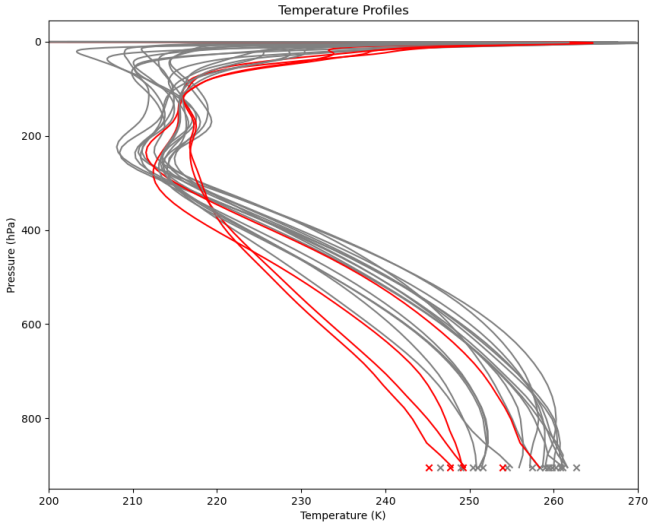

Figure 9: Average temperature profiles over the region of interest for each day 12th – 31st December plotted on a grid of pressure levels. The days flagged as 'high' methanol (24th – 27th December inclusive) are shown in red and the other days in grey. Crosses mark the surface temperature.

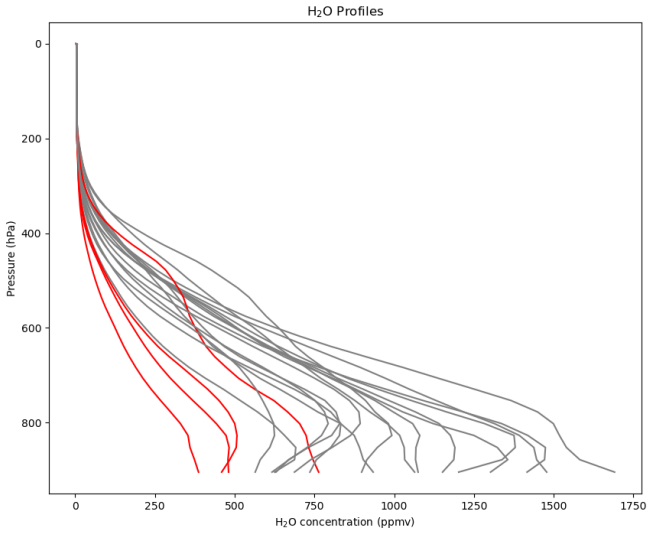

Figure 10: Average H_2O profiles over the region of interest with colours assigned as in Figure 9.

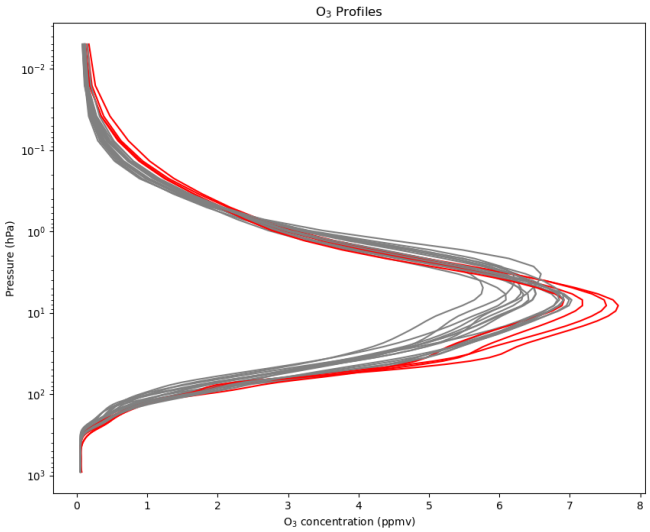

Figure 11: Average O_3 profiles over the region of interest with colours assigned as in Figure 9, plotted on a logarithmic scale of pressure.

4.3 Simulated spectra

4.3.1 Method

Noting both the high ozone concentration and the unfavourable thermal contrast between the lower troposphere and the surface on the days of the plume's appearance, we want to determine whether the atmospheric conditions are responsible for the SLR generating anomalous results.
The atmospheric profiles in the IASI L2 product [14] can be used to generate simulated spectra with the RFM [9]. The average profile for all the cloud-free pixels in the boxed region on each day in December was calculated and inputted through the RFM, to produce a simulated spectrum for each day in December. The RFM was run for an atmosphere that contained only O_3, H_2O and CO_2 (these are the only atmospheric gases with absorption in the spectral range of interest). We chose to model the atmospheric composition with no methanol at all, to test whether the same trend in x_s can be detected by the SLR for these conditions even when there is no methanol present.

4.3.2 Results

The resulting s and x_s values are plotted in blue in Figure 8. The temperature structure produces a decreased scale factor throughout December as expected, but the methanol column hovers near zero. This means the SLR is still working accurately for the average conditions for each day since zero methanol was inputted into the atmospheric composition for the RFM-simulated spectrum. This also indicates that the higher concentration of ozone is not causing an absorption feature that the SLR is misinterpreting in its SVD process, since the days with high

ozone (24th – 27th December) still produce a methanol column of less than 0.5×10^{-4} mol m^{-2}.
The simulated spectrum based on average profiles on 26th December was compared to the average spectrum (given by averaging all L1c spectra of individual pixels) in Figure 12. The RFM-modelled spectrum was simulated for an atmosphere containing no methanol so differencing the two spectra should give a methanol peak at 1034 cm^{-1}. No such significant peak is visible, further confirming that there is no methanol present.

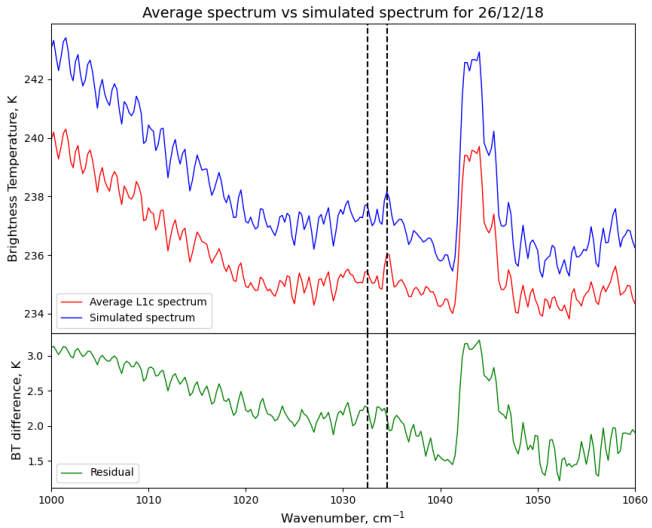

Figure 12: The averaged spectrum and the simulated spectrum for the boxed region are plotted over the spectral range of interest. The residual is plotted in the lower panel, with the dashed lines indicating the wavenumber at which we expect a methanol peak in the residual spectrum.

4.4 Influence of noise

4.4.1 Method

Having established that the SLR is generally well-behaved with noise-free spectra, we must now consider if the 'high' methanol values are due to noise. For a purely linear retrieval, we wouldn't expect the noise to shift the mean or median, but since the SLR involves dividing by the scale factor (which is often close to zero in unfavourable detection conditions), the non-linearity could be producing the anomalous shift to high x_s.
After creating the simulated spectra (on an atmosphere with zero methanol), a Gaussian-distributed noise vector centred on 0.2 K was added to each spectrum. This process was iterated 1000 times for each day; 1000 new noisy spectra were run through the SLR to obtain 1000 s and x_s values per day. We expect that adding noise under unfavourable detection conditions will recreate the variation and spread in methanol column x_s that we see in the original data (plotted in green in Figure 8.

4.4.2 Results

Adding noise to the simulated spectra causes a spike in the upper quartile of methanol column x_s on the days when the scale factor is lowest, as shown in Figure 13. This result means that in unfavourable detection conditions, such as those over Siberia in December 2018, a methanol column x_s below 2×10^{-4} mol m^{-2} is unreliable because instrument noise amplified by the scale factor could produce this value even when no methanol is present.

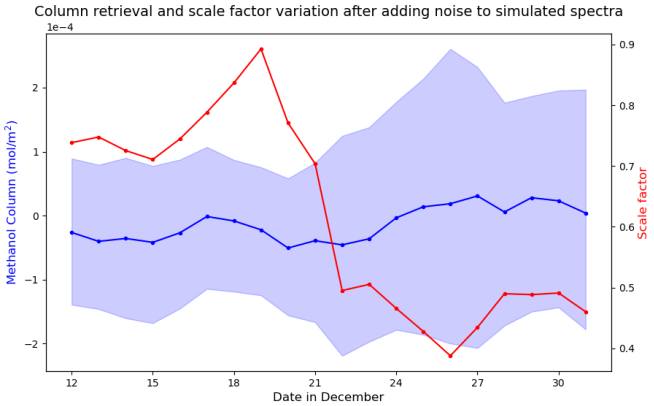

Figure 13: Variation of median methanol column (left axis) in blue and scale factor (right axis) in red found by running the SLR on 1000 simulated spectra with random noise added. The shaded region gives the inter-quartile range of the column retrieval.

Razavi et al. [2] came to a similar conclusion in their retrieval of methanol concentration from IASI spectra. They found that, due to its noise, the minimum total methanol column that can be detected by IASI was evaluated from simulations to be about 1.60×10^{16} molec cm^{-2} which is equivalent to 2.66×10^{-4} mol m^{-2}, and all IASI methanol retrievals below this magnitude are unreliable.
This spike in the upper quartile is still a factor of 4 times smaller than the original data plotted in green in Figure 8 which implies that the amplification of noise by a decreased scale factor may not be the sole cause of the false high columns. This simulated spectrum was modelled by the RFM on an atmosphere containing zero methanol. Since past research [2] found a typical methanol value for Siberia in mid-winter to be 2.5×10^{-4} mol m^{-2}, it would be useful to rerun the RFM with this low amount of methanol in the atmospheric composition, rather than zero. This may reproduce the trend and inter-quartile range shown in the original data plotted in green in Figure 8.

5 Conclusion

This project aimed to investigate the abundance of methanol detected by the SLR algorithm run on IASI spectra over Siberia in December 2018. We wanted to confirm whether or not the plume existed and, either

way, explain the cause of the readings of high concentration.

After completing preliminary tests, we concluded that the methanol plume was not present, but instead was caused by the anomalous behaviour of the SLR. Then, focusing on a small geographical region, the SLR was implemented on measured spectra individually, spectra with reduced noise due to averaging, and spectra with no noise that were simulated by the RFM. It was noted that the increase in methanol column value aligns with a decrease in the scale factor of the SLR algorithm which is due to a much colder surface temperature on these days. The days with a high methanol concentration also correspond with a high ozone concentration, a gas that has large absorption features in the same spectral range. However, producing simulated spectra from these ozone profiles and running the SLR on these showed that there was nothing anomalous in the atmospheric composition such as ozone that the singular vectors did not account for.

The test with noise added to a simulated spectrum showed that, under these unfavourable conditions, an atmosphere containing zero methanol gives readings with an upper quartile greater than 2×10^{-4} mol m^{-2}. This is in agreement with recent work by Razavi et al. [2] on IASI noise in methanol retrievals. A further investigation should be carried out which simulates spectra for a typical Siberian methanol level (2.5×10^{-4} mol m^{-2}) instead and monitors the spread of SLR readings after adding noise to the simulated spectra, to reproduce the original trend.

We can conclude that the high methanol readings are not caused by anomalous absorption features, but instead by a combination of two consequences of the reduced thermal contrast. This reduced contrast causes the low column of methanol to produce a tiny signature of the order of instrument noise and also generates a decreased scale factor in the SLR, which amplifies the peak non-linearly.

This investigation was limited by a few factors that offer room for improvement. Unlike the study [2] by Razavi et al., the emissivity of the surface wasn't taken into account and the behaviour of the SLR for varying emissivity is unknown. A better understanding of the surface emissivity would allow for more informed decisions when filtering pixels for this experiment.

Throughout December, the time at which the satellite passed over Siberia shifts from daytime to nighttime and during the night the surface temperature could be colder than the atmosphere, thus producing emission features in brightness temperature spectra. For more conclusive results, the pixels should be filtered by solar zenith angle for daytime measurements to ensure the spectra only contain absorption features. A study by Coheur et al. [6] into methanol over the Baikal region considers both emission and absorption features. The SLR only deals with absorption features as its singular vectors are generated for positive thermal contrasts, however, given the temperature structure, broadening the scope of the SLR to interpret emission features would be useful. This could be achieved by performing SVD on simulated spectra for reduced and inverted thermal contrasts.

References

[1] EUMETSAT. *Metop Series*. https://www.eumetsat.int/our-satellites/metop-series. Accessed: 11/02/2024.

[2] A. Razavi et al. "Global distributions of methanol and formic acid retrieved for the first time from the IASI/MetOp thermal infrared sounder". In: *Atmospheric Chemistry and Physics* 11.2 (2011), pp. 857–872. DOI: 10.5194/acp-11-857-2011.

[3] C. S. Moon. "Estimations of the lethal and exposure doses for representative methanol symptoms in humans". In: *Annals of occupational and environmental medicine* 29 (2017), p. 44. DOI: 10.1186/s40557-017-0197-5.

[4] I. E. Galbally and W. Kirstine. "The Production of Methanol by Flowering Plants and the Global Cycle of Methanol". In: *Journal of Atmospheric Chemistry* 43 (2002), pp. 195–229. ISSN: 1573-0662. DOI: https://doi.org/10.1023/A:1020684815474.

[5] K. H. Bates et al. "The Global Budget of Atmospheric Methanol: New Constraints on Secondary, Oceanic, and Terrestrial Sources". In: *Journal of Geophysical Research: Atmospheres* 126.4 (2021), e2020JD033439. DOI: https://doi.org/10.1029/2020JD033439.

[6] P.-F. Coheur et al. "IASI measurements of reactive trace species in biomass burning plumes". In: *Atmospheric Chemistry and Physics* 9.15 (2009), pp. 5655–5667. DOI: 10.5194/acp-9-5655-2009.

[7] T. Stavrakou et al. "First space-based derivation of the global atmospheric methanol emission fluxes". In: *Atmospheric Chemistry and Physics* 11.10 (2011), pp. 4873–4898. DOI: 10.5194/acp-11-4873-2011.

[8] EUMETSAT. *IASI Level 1: Product Guide*. https://www-cdn.eumetsat.int/files/2020-04/pdf_iasi_pg.pdf. Accessed: 12/02/2024.

[9] A. Dudhia. "The Reference Forward Model (RFM)". In: *Journal of Quantitative Spectroscopy and Radiative Transfer* 186 (2017). Satellite Remote Sensing and Spectroscopy: Joint ACE-Odin Meeting, October 2015, pp. 243–253. ISSN: 0022-4073. DOI: https://doi.org/10.1016/j.jqsrt.2016.06.018.

[10] A. Dudhia. *Oxford IASI Scaled Linear Retrievals*. https://eodg.atm.ox.ac.uk/IASI/slr/about.html. Accessed: 29/02/2024.

[11] S. L. Brunton and J. N. Kutz. "Singular Value Decomposition (SVD)". In: *Data-Driven Science and Engineering: Machine Learning, Dynamical Systems, and Control*. Cambridge University Press, 2019, pp. 3–46.

[12] A. F. Stein et al. "NOAA's HYSPLIT Atmospheric Transport and Dispersion Modeling System". In: *Bulletin of the American Meteorological Society* 96.12 (2015), pp. 2059–2077. DOI: 10.1175/BAMS-D-14-00110.1.

[13] RAL Space. *RAL Remote Sensing Group's Data Visualisation Portal*. https://gws-access.jasmin.ac.uk/public/rsg_share/webpages/rsg_data_viewer/. Accessed: 12/02/2024.

[14] EUMETSAT. *IASI Level 2: Product Guide*. https://user.eumetsat.int/s3/eup-strapi-media/IASI_Level_2_Product_Guide_8f61a2369f.pdf. Accessed: 01/03/2024.